CHAPTER 1

HUGS 2022 Lecture 1: Construction of QCD (Part 1)

1.1 Overview: The Theoretical Framework

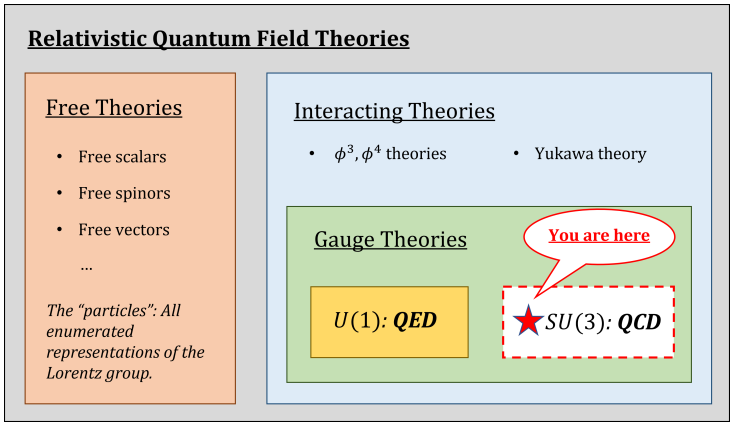

Figure 1.1: Illustration of QCD's place in the landscape of relativistic quantum field theories.

Quantum Field Theory

By way of introduction, let us begin by orienting ourselves with respect to the theoretical language and calculculational approach we will employ to describe QCD, as visualized in Fig. 1.1. The language of relativistic quantum mechanics is *quantum field theory* (QFT). QFT expresses the physics of multiparticle creation and annihilation in a manifestly Lorentz-covariant formalism, which elegantly solves the problem of causality for a relativistic quantum theory.

The simplest quantum theories are "free" theories – Lagrangians whose equations of motion are *linear*, such that the solutions obey a noninteracting

superposition principle. These free theories define the "particles," with one Lorentz-invariant Lagrangian that can be enumerated for each representation of the Lorentz group $SO^+(3,1)$. More complex Lagrangians with nonlinear equations of motion are interpreted as *interactions* among the particles. The "traditional" approach to solving interacting theories is *perturbation theory*: a Taylor series expansion of physical observables in terms of a small coupling constant, such as the fine structure constant $\alpha_{EM} \approx 1/137$ in quantum electrodynamics (QED). This allows for a systematic order-by-order computation of observables with controllable error in QFT.

Perturbative and Nonperturbative Effects

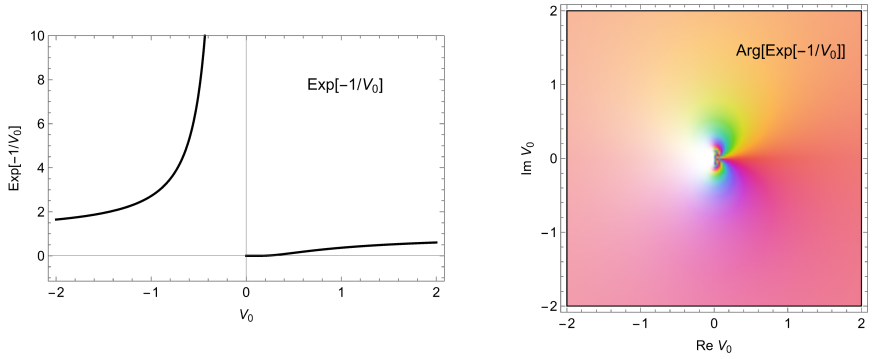

Figure 1.2: Behavior of the essential singularity $\exp[-1/V_0]$ in the complex plane.

Perturbation theory is a powerful, systematic approach to studying interacting theories, but it is not complete. The fundamental philosophy is an expansion of observables in a smooth Taylor series at small values of the coupling constant. The assumed smoothness of this expansion can fail in a number of important ways. First, there can be fundamental physics effects which are essentially *nonperturbative* in nature. Nonperturbative effects are often associated with a radical realignment of the degrees of freedom in a system which causes perturbation theory to break down. One famous example is nonperturbative transition from degrees of freedom resembling electrons and holes in a normal metal to Cooper pairs in a superconductor. As computed in the BCS theory of superconductivity, the binding energy E_b of a Cooper pair is

$$E_b = 2\omega_D \, e^{-2/V_0 \rho(\varepsilon_F)} \,, \tag{1.1}$$

where V_0 is the strength of the effective potential between two electrons, ω_D is the Debye frequency and $\rho(\varepsilon_F)$ is the density of states at the Fermi energy[1]. Rather

[1] For more information, see these nice lecture notes.

than having a well-behaved Taylor series at weak coupling $V_0 \to 0$, the binding energy (1.1) instead has an essential singularity of the form $f(V_0) = e^{-1/V_0}$ shown in Fig. 1.2. This form, which often occurs in nonperturbative mechanisms, *has no Taylor series*:

$$\begin{aligned} f(V_0) &\stackrel{?}{=} f(V_0 = 0) + V_0 \left.\frac{df}{dV_0}\right|_{V_0=0} + \frac{1}{2}V_0^2 \left.\frac{d^2 f}{dV_0^2}\right|_{V_0=0} + \cdots \\ &\stackrel{!}{=} 0 + 0 + 0 + \cdots . \end{aligned} \tag{1.2}$$

A perturbative calculation of the binding energy (1.1) would yield *zero, to all orders in perturbation theory* and could never discover the superconducting phase transition. Likewise, one can construct a "proof" that $E_b = 0$ to all orders in perturbation theory, but this still misses the possibility of nonperturbative contributions.

This example illustrates that while perturbation theory can capture the smooth evolution of the degrees of freedom in a quantum field theory, by construction it cannot capture a severe rupture in those degrees of freedom such as during a phase transition. Exactly the same kind of mechanism (1.1) which leads to the formation of a Cooper-pair condensate and the superconducting phase transition in BCS theory is also responsible for the spontaneous breaking of chiral symmetry in QCD, which is associated with quark confinement and the emergence of the proton mass.

Asymptotic Series in Perturbation Theory

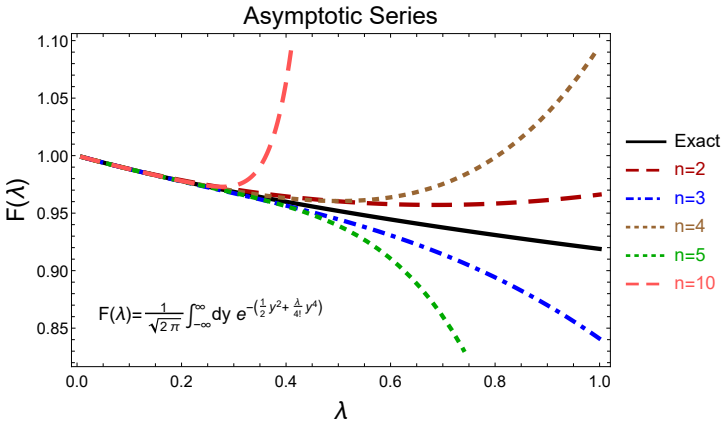

Figure 1.3: One example of the breakdown of convergence in an asymptotic series.

Another important caveat to the applicability of perturbation theory is the fact that the *perturbation series does not converge* in general. Rather than

producing an absolutely-convergent series, the perturbation expansion is an asymptotic series. This means that, while a fixed-order calculation may provide a good estimate of the true solution, the accuracy of that estimate does not necessarily increase as one goes to higher orders. An example of an asymptotic series is shown in Fig. 1.3. Note that the fixed-order approximation gets better as one increases the accuracy from LO, to NLO ($n = 2$), to NNLO ($n = 3$). But as one pushes the perturbative expansion to higher and higher orders, the *error starts to increase* rather than decrease. The $n = 5$ curve is clearly worse than the $n = 3$ curve, and the $n = 10$ curve is a terrible approximation to the exact solution. This illustrates that, sometimes, "working harder" (computing to higher accuracy in the perturbation series) doesn't always pay off.

Resummation in Perturbation Theory

Finally, there can be a more gradual evolution of the degrees of freedom in a quantum system which **is** capturable in perturbation theory. This often occurs when there is a systematic enhancement of certain amplitudes due to a logarithmically large phase space, for instance in integrals of the form

$$\alpha \int_{\Lambda^2}^{E^2} \frac{dk_\perp^2}{k_\perp^2} = \alpha \ln \frac{E^2}{\Lambda^2} \text{ , or} \tag{1.3a}$$

$$\alpha \int_{\Lambda/E}^{1} \frac{dz}{z} = \alpha \ln \frac{E}{\Lambda} \, . \tag{1.3b}$$

This creates an interesting tension where the weak-coupling approximation $\alpha \ll 1$ may still be valid, but certain amplitudes are systematically enhanced by a large logarithm $\ln E/\Lambda$ coming from the limits of the phase space. If that logarithm becomes large enough, it can begin to compete with the smallness of the coupling α. In the limit

$$\alpha \ll 1 \qquad , \qquad \ln \frac{E}{\Lambda} \gg 1 \qquad , \qquad \alpha \ln \frac{E}{\Lambda} \sim \mathcal{O}(1) \, , \tag{1.4}$$

these systematically enhanced diagrams are not "small" at all, and we must *re-sum them all*, since

$$1 \sim \alpha \ln \frac{E}{\lambda} \sim \left(\alpha \ln \frac{E}{\lambda} \right)^2 \sim \left(\alpha \ln \frac{E}{\lambda} \right)^3 \sim \cdots \sim \left(\alpha \ln \frac{E}{\lambda} \right)^n \, . \tag{1.5}$$

Resumming these large logarithmic corrections can be accomplished by expressing them as a differential equation; if that equation can be solved, then its solution encodes the iteration of these enhanced corrections to all orders in perturbation theory. This procedure re-orders the perturbation series, giving the *leading-logarithmic approximation* (LLA) to the resummation. This description of a gradual transformation of degrees of freedom in QFT is often

referred to as *quantum evolution*. It occurs prominently in QCD in several forms, including the DGLAP evolution with Q^2 and BFKL evolution with x_B of parton distribution functions.

1.2 Gauge Theory of $U(1)$: Quantum Electrodynamics

The Golden Archetype of Gauge Symmetry

Quantum Electrodynamics (QED) is defined by the Lagrangian

$$\mathcal{L}_{QED} = \bar{\psi}(i\not{\partial} - m)\psi - \frac{1}{4}F_{\mu\nu}F^{\mu\nu} - e\bar{\psi}\gamma_\mu\psi\, A^\mu \,, \tag{1.6}$$

which describes the interactions of charged fermions ("electrons") with vector bosons ("photons"). QED is a *gauge theory*, meaning that the particular *form of the photon/electron interaction vertex is uniquely dictated* by a symmetry transformation (called a "gauge symmetry") of the Lagrangian (1.6). The gauge symmetry is not a quirk of QED; it is an essential feature necessary to even define an interacting vector boson.

Global Symmetry and Conserved Current

The QED Lagrangian (1.6) is uniquely obtained from the free Dirac Lagrangian

$$\mathcal{L}_{Dirac} = \bar{\psi}(i\not{\partial} - m)\psi \tag{1.7}$$

through the process of *minimal coupling*. The free Dirac Lagrangian (1.7) is invariant under the global symmetry transformation

$$\psi'(x) = e^{i\phi}\psi(x) \qquad \text{or} \qquad \begin{bmatrix} \mathrm{Re}\,\psi'(x) \\ \mathrm{Im}\,\psi'(x) \end{bmatrix} = \begin{bmatrix} \cos\phi & -\sin\phi \\ \sin\phi & \cos\phi \end{bmatrix} \begin{bmatrix} \mathrm{Re}\,\psi(x) \\ \mathrm{Im}\,\psi(x) \end{bmatrix} \,, \tag{1.8}$$

where ϕ is an arbitrary constant. This symmetry transformation is just a complex phase rotation, which may be regarded as a "1×1 unitary matrix". This describes the Lie group $U(1)$, which is a global symmetry of the free Dirac Lagrangian (1.7). Since charge conjugation $\psi \leftrightarrow \bar{\psi}$ changes particles into antiparticles, this $U(1)$ rotation may be regarded as a continuous rotation which redefines the particles and antiparticles.

By Noether's theorem, the invariance of the Lagrangian (1.7) under the continuous symmetry transformation (1.8) implies the existence of a conserved current:

$$\begin{aligned} \delta\mathcal{L} = 0 &= \frac{\delta\mathcal{L}}{\delta\psi}\delta\psi + \delta\bar{\psi}\frac{\delta\mathcal{L}}{\delta\bar{\psi}} + \frac{\delta\mathcal{L}}{\delta(\partial_\mu\psi)}\delta(\partial_\mu\psi) \\ &= \left(\partial_\mu \frac{\delta\mathcal{L}}{\delta(\partial_\mu\psi)}\right)\delta\psi + \frac{\delta\mathcal{L}}{\delta(\partial_\mu\psi)}\partial_\mu(\delta\psi) \\ &= \partial_\mu\left(\frac{\delta\mathcal{L}}{\delta(\partial_\mu\psi)}\delta\psi\right) \\ 0 &= \partial_\mu\left(\bar{\psi}\gamma^\mu\psi\right) \end{aligned} \tag{1.9}$$

where we have used the equations of motion. The *net particle number current* is conserved:

$$j^\mu = \bar{\psi}\gamma^\mu\psi \qquad , \qquad \partial_\mu j^\mu = 0\,, \tag{1.10}$$

reflecting the conservation of electric charge. The electromagnetic current $J^\mu_{EM} = e\bar{\psi}\gamma^\mu\psi$ is just the particle number current, weighted by the charge.

The Problem with Vector Bosons: Scalar Polarization Mode

The form of the QED interaction vertex (1.6) is of the form

$$\mathcal{L}_I = -J^\mu_{EM} A_\mu = -e\bar{\psi}\gamma^\mu\psi\, A_\mu, \tag{1.11}$$

which introduces the photon field A^μ as being *created by the conserved current* j^μ. This choice of vertex directly links the properties of the conserved current j^μ produced by the $U(1)$ global symmetry and the structure of the vector field A^μ. This is not just a curiosity; it is an essential feature necessary for the photon field A^μ to be well-defined at all. The reason is that, in 4-dimensional spacetime, there are potentially four independent polarization modes of A^μ, including the "timelike" or "scalar polarization" mode, which can be written as the gradient of a scalar field:

$$A^\mu_{(scalar)}(x) = \partial^\mu\phi(x)\,. \tag{1.12}$$

The timelike polarization is "unphysical" – if quantized, it would lead to states of negative norm, which are incompatible with a Hilbert space of quantum states. Getting rid of the sick scalar polarization is essential for any self-consistent quantum theory of vector bosons.

An interaction vertex of the form (1.11) which couples the vector boson to a *conserved* current arising from a global symmetry eliminates the scalar-polarized modes (1.12) in an elegant way: by reducing them to a *symmetry transformation* on the Lagrangian. If we shift A^μ by the addition of a scalar-polarized mode,

$$A'^\mu(x) = A^\mu(x) + \partial^\mu\phi(x) \tag{1.13a}$$

$$\mathcal{L}'_I = \mathcal{L}_I - ej^\mu\partial_\mu\phi = \mathcal{L}_I - \partial_\mu(ej^\mu\phi) \tag{1.13b}$$

the interaction term is *invariant* (up to an irrelevant total derivative). Thus, with a special interaction vertex of the form (1.11), the scalar modes are removed as "redundant, unphysical degrees of freedom" which have no consequence on observables.

CHAPTER 2

HUGS 2022 Lecture 2: Construction of QCD (Part 2)

2.1 Previously

- Taxonomy of quantum field theories: free theories, interacting theories, gauge theories
- Perturbation theory and its limitations
- Global symmetry and current conservation
- Problematic scalar-polarized mode of the vector field A^μ

Minimal Coupling: Gauging the QED Lagrangian

The extension of the free Dirac Lagrangian (1.7) to include the *minimal coupling* to the vector field A^μ through a term of the form $-j_\mu A^\mu$ can be compactly expressed using the *gauge-covariant derivative*:

$$\begin{aligned}\mathcal{L}_{gauged} &= \bar{\psi}(i\gamma_\mu\partial^\mu - m)\psi - e\,\bar{\psi}\gamma_\mu\psi\,A^\mu \\ &= \bar{\psi}[i\gamma_\mu(\partial^\mu + ie\,A^\mu) - m]\psi \\ &\equiv \bar{\psi}(i\not{D} - m)\psi\,. \end{aligned} \tag{2.1}$$

The remarkable physics of extending the local $U(1)$ symmetry to form the basis of a local $U(1)$ gauge theory is encoded in the simple replacement of the partial derivative with the covariant derivative:

$$\partial_\mu \to D_\mu \equiv \partial_\mu + ie\,A_\mu\,. \tag{2.2}$$

The covariant derivative expresses the fact that the shift (1.13) of A^μ by the addition of a scalar mode is now interconnected with the $U(1)$ symmetry of the Dirac Lagrangian (1.7). Under the more general version of the transformation (1.8) in which the rotation phase $\phi(x)$ can vary as a function of spacetime,

$$\psi'(x) = e^{i\phi(x)}\psi(x)\,, \tag{2.3}$$

the Lagrangian (2.1) transforms as

$$\begin{aligned}\mathcal{L}'(x) &= \bar{\psi}'(x)(i\gamma_\mu\partial^\mu - m)\psi'(x) - e\,\bar{\psi}'(x)\gamma_\mu\psi'(x)\,A^{\mu\,\prime}(x) \\ &= \bar{\psi}(x)\,e^{-i\phi(x)}(i\gamma_\mu\partial^\mu - m)e^{i\phi(x)}\,\psi(x) - e\,\bar{\psi}(x)\,e^{-i\phi(x)}\gamma_\mu e^{i\phi(x)}\,\psi(x)\,A^{\mu\,\prime}(x) \\ &= \bar{\psi}(x)(i\gamma_\mu\partial^\mu - m)\psi(x) - \bar{\psi}(x)\gamma_\mu\psi(x)\,\partial^\mu\phi(x) - e\,\bar{\psi}(x)\gamma_\mu\psi(x)\,A^{\mu\,\prime}(x) \\ &= \bar{\psi}(x)(i\gamma_\mu\partial^\mu - m)\psi(x) - e\,\bar{\psi}(x)\gamma_\mu\psi(x)\left[A^{\mu\,\prime}(x) + \frac{1}{e}\partial^\mu\phi(x)\right]. \qquad (2.4)\end{aligned}$$

The effect of the *local* transformation (2.3) can be interpreted as *shifting* A^μ *by a scalar-polarized mode*, exactly as we did in Eq. (1.13). Since the minimal coupling of A^μ to the conserved current $j_m u$ guarantees that a shift by a scalar mode is an unphysical symmetry transformation, the two pieces (global $U(1)$ symmetry and scalar polarizations of $A_m u$) work in tandem as part of a single composite symmetry operation known as *gauge symmetry.*

Choosing a special interaction vertex of the form (1.11) has united the elimination of the scalar-polarized mode with the global $U(1)$ symmetry responsible for the conserved current j^μ. This choice effectively *enlarges the* $U(1)$ *symmetry group* from a global symmetry to a local symmetry and uses it to *define the photon* field A^μ. Without a gauge-invariant coupling of this form, the photon field *could not exist at all*, since it would be polluted with unworkable scalar-polarized modes.

Geometric Interpretation

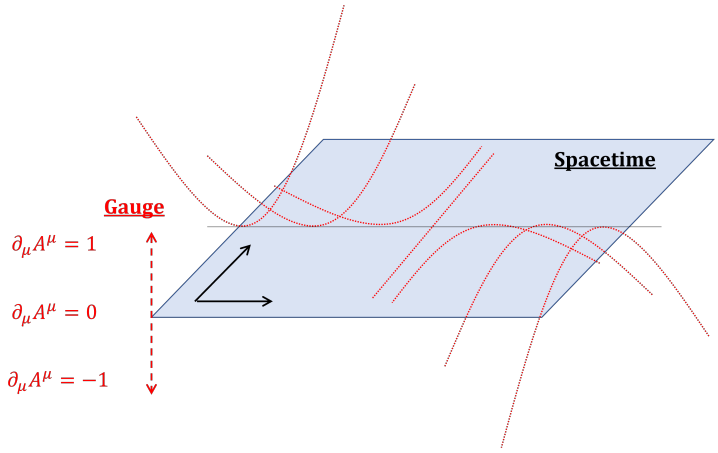

Figure 2.1: Sketch of the combined spacetime + gauge manifold.

From the point of view of the local gauge transformation (2.3), the covariant derivative (2.2) has a natural geometric interpretation. The ordinary partial derivative ∂_μ is not invariant under the local $U(1)$ transformation (2.3), because different points x^μ of spacetime transform differently, so the partial derivative

makes an unequal comparison between two adjacent points. The covariant derivative (2.2) *compensates* for the different transformations of $\psi(x)$ at different points, permitting a simple meaningful (gauge-invariant) comparison between two points.

Under the combined transformation

$$\psi'(x) = e^{i\phi(x)}\psi(x)\,, \tag{2.5a}$$

$$A^{\mu\,\prime}(x) = A^{\mu}(x) - \frac{1}{e}\partial^{\mu}\phi(x)\,, \tag{2.5b}$$

the covariant derivative transforms as

$$\begin{aligned}\big(D_\mu\psi(x)\big)' &\equiv (\partial_\mu + ie\,A'_\mu)\,\psi'(x)\\ &= (\partial_\mu + ie\,A_\mu - i\partial_\mu\phi)\,e^{i\phi(x)}\psi(x)\\ &= e^{i\phi(x)}(\partial_\mu + ie\,A_\mu)\psi(x)\\ &= e^{i\phi(x)}\,D_\mu\psi(x)\,.\end{aligned} \tag{2.6}$$

That is: *the covariant derivative of a field has the same gauge transformation as the field itself.* This is the precise mathematical statement that the covariant derivative *cancels the nonlocal differences in the gauge transformation*, providing a meaningful way to compare two different points in spacetime in a gauge-invariant way. For instance, it is clear that $\bar{\psi}D_\mu\psi$ is gauge invariant.

We have found that, by minimally coupling the photon field to the conserved electric current, we have constructed a Lagrangian (2.1) which is invariant under a *mix* of Lorentz transformations and shifting A^μ by scalar modes. Even though spacetime itself is "flat" (in this discussion), the different transformations of neighboring points under a local $U(1)$ transformation act as if the *combined* spacetime + gauge manifold is *curved*. From this point of view, the problem of how to compute meaningful derivatives on a curved manifold is a standard one in differential geometry. The covariant derivative (2.2) precisely introduces the photon field A_μ as a metric connection which compensates for the curvature of the gauge dimensions along the physical spacetime dimensions.

Field-Strength Tensor as a Generalized Curl

The last piece of the QED Lagrangian (1.6) is the kinetic term associated with the free photon field. The free-field Lagrangian for A^μ must be quadratic in A, coupled to derivatives to contain momenta, and a Lorentz scalar. It must be massless, as an essential requirement of gauge symmetry[1]. From these considerations, the kinetic term can be deduced to be

$$\mathcal{L}_{kinetic} = -\frac{1}{4}F_{\mu\nu}F^{\mu\nu}\,, \tag{2.7}$$

[1]Massive vector bosons have a different relation with their scalar-polarized modes, whose removal is generally enforced by constraint.

where the antisymmetric field-strength tensor $F_{\mu\nu} = \partial_\mu A_\nu - \partial_\nu A_\mu$ is a four-dimensional generalization of the curl, transforming as an antisymmetric rank-2 tensor under Lorentz tranformations.

Based on the geometric interpretation of gauge transformations discussed previously, we expect that this generalized curl should also have a sensible interpretation under gauge transformations. Indeed, the field-strength tensor $F^{\mu\nu}$ has a particularly simple expression in terms of the covariant derivative (2.2):

$$\begin{aligned} \Big[D_\mu\,,\,D_\nu\Big] &= ie(\partial_\mu A_\nu - \partial_\nu A_\mu) = ie\,F_{\mu\nu} \\ \therefore \qquad F_{\mu\nu} &= \frac{-i}{e}\Big[D_\mu\,,\,D_\nu\Big]\,. \end{aligned} \tag{2.8}$$

This expression, as a commutator of covariant derivatives, describes the generalized curl *including the curvature along the gauge direction.* Since D_μ is itself a gauge-covariant quantity (transforming locally under gauge transformations), so is $F_{\mu\nu}$. In the case of QED, $F_{\mu\nu}$ is simply gauge-invariant, but in the more general case, $F_{\mu\nu}$ may transform under gauge transformations, and its transformation properties are dictated by those of the covariant derivative D_μ.

Next Steps

Taken together, the QED Lagrangian

$$\mathcal{L}_{QED} = \bar{\psi}(i\partial\!\!\!/ - m)\psi - \frac{1}{4}F_{\mu\nu}F^{\mu\nu} - e\bar{\psi}\gamma_\mu\psi\,A^\mu\,, \tag{2.9}$$

and all the physics of electrodynamics are consequences of a single unifying principle: $U(1)$ gauge symmetry. Physically, this gauge group encodes the statement that *electric charge is a scalar quantity.* Electric charge may be positive or negative (electrons and positrons), but it has no "direction" associated with it. This is reflected in the fact that $U(1)$ corresponds to rotation by a complex phase, without any matrix dimension to it. In a different gauge group, such as $SU(2)$ (the Pauli matrices), the gauge transformation could employ a nontrivial matrix structure. This single difference is responsible for the enormous complexity of QCD.

CHAPTER 3

HUGS 2022 Lecture 3: Construction of QCD (Part 3)

3.1 Previously

- Minimal coupling and the covariant derivative
- Enlarged local gauge symmetry on a combined gauge + spacetime manifold
- Gauge symmetry is **mandatory** for a massless vector boson like the photon to exist at all
- Gauge symmetry dictates the structure and physics of the Lagrangian at a very deep level.

3.2 Quantum Chromodynamics: Gauge Theory of $SU(3)$

Given the context developed thus far for what a gauge theory looks like in the case of the *Abelian* (commutative) gauge group $U(1)$, we can now state concisely what the governing principle of Quantum Chromodynamics (QCD) is. QCD is the $SU(3)$ gauge theory describing interactions of fermions called "quarks" with vector gauge bosons called "gluons."

Physically, the statement that the gauge group is $SU(3)$ implies that the quarks possess a new kind of charge quantum number, termed "color charge," which come in three different varieties, referred to as "red, blue, and green." The fact that the color quantum number comes in multiple independent types, or means that unlike electric charge, color charge carries a particular "direction" to it. Color charge is a *vector*[1]. This structural change in the gauge theory leads to profound differences between QED and QCD, as illustrated in Fig. **??**.

As with QED, we construct the QCD Lagrangian by starting with the free Dirac Lagrangian. Now we posit that there are three independent varieties of

[1] under $SU(3)$ transformations

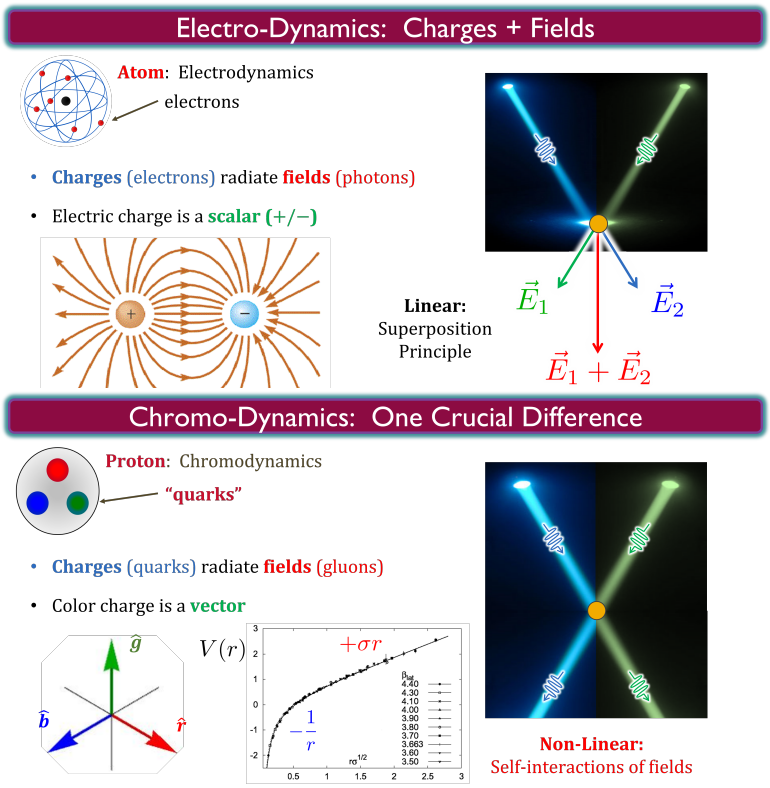

Figure 3.1: Comparison of the role of "charge" in QED versus QCD.

noninteracting fermions (quarks), corresponding to the three color states:

$$\mathcal{L}_{free} = \bar{\psi}_i(i\partial\!\!\!/ - m)\psi_i \qquad , \qquad i = 1, 2, 3\,. \tag{3.1}$$

Here we use indices like i, j, k to denote quark colors, referred to as the "fundamental representation" of $SU(3)$. The multicomponent Lagrangian (3.1) contains a much larger global symmetry than just the $U(1)$ symmetry of QED. It possesses a symmetry of *rotations among the 3 color states*. Just as the unitary rotation operator is given by $e^{i\vec{\phi}\cdot\vec{J}}$, with $\vec{\phi}$ the angle and axis of rotation and $\vec{J}$ the generators of rotations (angular momenta), the $SU(3)$ color rotations take a similar form:

$$\psi_i'(x) = \exp\left[i\phi^a t^a\right]_{ij}\, \psi_j(x) \qquad , \qquad a = 1, 2, \cdots, 8\,. \tag{3.2}$$

As with the rotation matrix, there are various rotation angles ϕ^a and $SU(3)$ rotation generators t^a, for each of the possible "axes of rotation" which can mix between the various color states. There are many such "axes" – in fact, there are more axes than the number of quark colors themselves. To go from any of

3 colors initially to any of 3 final colors, there are in principle $3^2 = 9$ possible axes of rotation. The group $SU(3)$ excludes the contribution proportional to the identity matrix[2], reducing the number to $3^2 - 1 = 8$ types of $SU(3)$ color rotations.

Group Structure of $SU(3)$

The nomenclature $SU(3)$ for the QCD gauge group refers to the group of *special, unitary,* 3×3 *matrices* which perform the color rotations among the quark colors. The term "special" indicates that the matrices have *unit determinant*, which is the condition that excludes the unit matrix ("QCD photon").

The 8 generators of $SU(3)$ in QCD are written

$$t^a = \frac{1}{2}\lambda^a \tag{3.3}$$

where λ^a are the Gell-Mann matrices

$$\lambda^1 = \begin{bmatrix} & 1 & \\ 1 & & \\ & & \end{bmatrix} \qquad \lambda^2 = \begin{bmatrix} & -i & \\ i & & \\ & & \end{bmatrix} \qquad \lambda^3 = \begin{bmatrix} 1 & & \\ & -1 & \\ & & \end{bmatrix}$$

$$\lambda^4 = \begin{bmatrix} & & 1 \\ & & \\ 1 & & \end{bmatrix} \qquad \lambda^5 = \begin{bmatrix} & & -i \\ & & \\ i & & \end{bmatrix} \qquad \lambda^6 = \begin{bmatrix} & & \\ & & 1 \\ & 1 & \end{bmatrix}$$

$$\lambda^7 = \begin{bmatrix} & & \\ & & -i \\ & i & \end{bmatrix} \qquad \lambda^8 = \frac{1}{\sqrt{3}} \begin{bmatrix} 1 & & \\ & 1 & \\ & & -2 \end{bmatrix} \quad . \tag{3.4}$$

In this fundamental representation of $SU(3)$, the Gell-Mann matrices are these explicit 3×3 matrices, with the particular components t^3, t^8 being diagonal. The essential property of $SU(3)$ is the Lie algebra of its generators, which can be expressed through the commutator relation

$$[t^a\,,\, t^b] = i f^{abc}\, t^c\,, \tag{3.5}$$

where f^{abc} are the totally antisymmetric structure constants

f^{abc}	1	$\frac{1}{2}$	$-\frac{1}{2}$	$\frac{1}{2}$	$\frac{1}{2}$	$\frac{1}{2}$	$-\frac{1}{2}$	$\frac{\sqrt{3}}{2}$	$\frac{\sqrt{3}}{2}$
a	1	1	1	2	2	3	3	4	6
b	2	4	5	4	5	4	6	5	7
c	3	7	6	6	7	5	7	8	8

(3.6)

with $f^{abc} = -f^{bac} = -f^{acb}$ and all other components of f^{abc} equal to zero.

The structure constants f^{abc} themselves provide the 8-dimensional "adjoint representation" of $SU(3)$ (which we denote here in capital letters),

$$(T^a)_{bc} \equiv -i\, f^{abc}\,, \tag{3.7}$$

[2]This would resemble the interaction of the photon, since it would again be a $U(1)$ gauge subgroup.

which satisfies the Lie (commutator) algebra (3.5)

$$[T^a\,,\,T^b] = if^{abc}\,T^c \tag{3.8}$$

through the use of the Jacobi identity

$$\big[T^a\,,\,[T^b,T^c]\big] + \big[T^b\,,\,[T^c,T^a]\big] + \big[T^c\,,\,[T^a,T^b]\big] = 0\,. \tag{3.9}$$

Just as the 3×3 fundamental representation of $SU(3)$ describes the color states of the quarks and how they transform, the 8×8 adjoint representation describes the color states and interactions of the *gluons*.

Comparison to $SU(2)$

The Gell-Mann matrices (3.4) bear a clear resemblance to the Pauli matrices – for good reason. The Pauli matrices

$$\sigma^1 = \begin{bmatrix} & 1 \\ 1 & \end{bmatrix} \qquad \sigma^2 = \begin{bmatrix} & -i \\ i & \end{bmatrix} \qquad \sigma^3 = \begin{bmatrix} 1 & \\ & -1 \end{bmatrix} \tag{3.10}$$

define the generators $t^a = \frac{1}{2}\sigma^a$ (with $a = 1,2,3$) for the sister group $SU(2)$. The Lie algebra of $SU(2)$ is

$$[t^a\,,\,t^b] = i\epsilon^{abc}\,t^c\,, \tag{3.11}$$

where the structure constants for $SU(2)$ are just the elements of the antisymmetric Levi-Civita symbol.

In QCD, the quantum number for quark colors comes in 3 distinct states, giving the 3×3 Gell-Mann matrices (3.4). For the sister group $SU(2)$, the quantum number comes in 2 distinct states (usually in the context of "spin-up" and "spin-down"), giving the 2×2 Pauli matrices (3.10). For $SU(2)$, there are $2^2-1=3$ Pauli matrices, which correspond to the 3 independent *axes of rotation* $\sigma_x,\sigma_y,\sigma_z$. In the same way, the $3^2-1=8$ Gell-Mann matrices describe the *axes of (color) rotation* in QCD. With this analogy, we may speak of a rotation of a quark from fundamental color state (say) "red" ($i=1$) to "blue" ($j=2$) by the emission/absorption of a gluon in the adjoint color state $a=1$. This rotation would be described by the element $(\lambda^1)_{21}=1$ of the corresponding Gell-Mann matrix. This is what is meant by the statement "charge is a vector" in QCD.

The t'Hooft Large-N_c Limit

While for true QCD the number of quark colors is 3, the general gauge structure of QCD is only minimally modified for the case of arbitrary number of quark colors N_c. We have already benefited from the comparison of QCD ($N_c=3$) with the Pauli matrices of $N_c=2$. In fact, the algebra of the general gauge group $SU(N_c)$ becomes significantly *simpler* with clever usage of the number of colors N_c. One particularly powerful usage is the **t'Hooft large-N_c limit**

$$\alpha_s \to 0\,, \tag{3.12a}$$

$$N_c \to \infty \,, \tag{3.12b}$$

$$\alpha_s N_c = \text{const} \ll 1 \,. \tag{3.12c}$$

In this limit, the "S" of $SU(N_c)$ essentially becomes irrelevant (reducing $SU(N_c)$ to $U(N_c)$), since the one omitted generator is negligible compared to the $N_c^2 - 1 \approx N_c^2$ generators retained as $N_c \to \infty$. This can be clearly seen in the form of the Fierz identity for $SU(N_c)$

$$(t^a)^i{}_j \, (t^a)^k{}_\ell = \frac{1}{2}\delta^i{}_\ell \, \delta^k{}_j - \frac{1}{2N_c}\delta^i{}_j \, \delta^k{}_\ell \overset{N_c \gg 1}{\approx} \frac{1}{2}\delta^i{}_\ell \, \delta^k{}_j \,, \tag{3.13}$$

where the subtraction term enforcing $(t^a)^i{}_i = 0$ drops out.

In the large-N_c limit, the number of gluons $N_c^2 - 1$ far exceeds the number of quarks N_c, so this limit *simplifies QCD to effectively contain only gluons*. For gluon-dominated phenomena like small-x gluon saturation, this approximation is an especially powerful simplification. The simplified Fierz identity (3.13) allows the adjoint color flow of gluons to be replaced with an equivalent fundamental color flow, as if the gluon were being replaced by a quark-antiquark pair[3]. Moreover, the Feynman diagrams which dominate the large-N_c limit are always *planar*, meaning that (in a graph theory sense), all the vertices and propagators can be laid out flat on a plane, without any lines needing to cross "underneath" each other to construct the diagram. This can lead to a tremendous simplification of the color structure and associated operators for high-energy scattering in QCD, making the large-N_c limit highly advantageous in QCD. As an approximation to QCD, corrections to the large-N_c limit in real QCD often occurs at $\mathcal{O}\left(1/N_c^2\right)$ for physical observables. One would accordingly expect that the large-N_c limit is accurate at the level of $1/9 \sim 10\%$; however, for many observables, the large-N_c limit works even better in practice than this naive estimate.

3.3 Gauging the QCD Lagrangian

With the structure of $SU(N_c)$ in hand, we have all the ingredients we need to construct the QCD Lagrangian following the template of QED. Since the free multicomponent Dirac Lagrangian (3.1) is invariant under global $SU(N_c)$ color rotations (3.2), we have

$$\begin{aligned}
\delta\mathcal{L} = 0 &= \frac{\delta\mathcal{L}}{\delta\psi_i}\delta\psi_i + \delta\bar{\psi}_i\frac{\delta\mathcal{L}}{\delta\bar{\psi}_i} + \frac{\delta\mathcal{L}}{\delta(\partial_\mu\psi_i)}\delta(\partial_\mu\psi_i) \\
&= \left(\partial_\mu\frac{\delta\mathcal{L}}{\delta(\partial_\mu\psi_i)}\right)\delta\psi_i + \frac{\delta\mathcal{L}}{\delta(\partial_\mu\psi_i)}\partial_\mu(\delta\psi_i) \\
&= \partial_\mu\left(\frac{\delta\mathcal{L}}{\delta(\partial_\mu\psi_i)}\delta\psi_i\right)
\end{aligned}$$

[3]Caution: this statement applies only to the color representation, not to any other quantum numbers such as spin.

$$
\begin{aligned}
&= \partial_\mu \left(-\bar{\psi}_i \gamma^\mu \phi^a (t^a)_{ij} \psi_j\right) \\
\therefore \qquad 0 &= \partial_\mu \left(\bar{\psi}_i \gamma^\mu (t^a)_{ij} \psi_j\right) \ , \qquad (3.14)
\end{aligned}
$$

which gives a conserved color current

$$
j^{\mu a} \equiv \bar{\psi} \gamma_\mu t^a \psi \qquad (3.15)
$$

for each of the $a = 1, \ldots, (N_c^2 - 1)$ possible "axes" of color rotation.

With the conserved currents, we can introduce the gluon field $A^{\mu a}$ by minimally coupling it to the free Lagrangian (3.1). Adding the term $g {j_\mu}^a A^{\mu a}$ with g the QCD coupling renders the scalar modes of $A^{\mu a}$ unphysical symmetry transfromations, constructing the Lagrangian

$$
\begin{aligned}
\mathcal{L}_{gauged} &= \bar{\psi}(i\partial\!\!\!/ - m)\psi + g\bar{\psi}\gamma_\mu t^a \psi \, A^{\mu a} \\
&= \bar{\psi}\Big(i\gamma_\mu \left(\partial^\mu - igA^{\mu a} t^a\right) - m\Big)\psi \\
&= \bar{\psi}\Big(iD\!\!\!/ - m\Big)\psi \ , \qquad (3.16)
\end{aligned}
$$

where we have defined the gauge-covariant derivative

$$
D_\mu \equiv \partial_\mu - igA^a_\mu t^a \ . \qquad (3.17)
$$

For the Lagrangian (3.16) to be gauge invariant, the covariant derivative (3.17) must cancel the additional terms entering from a local gauge transformation. That is, the covariant derivative must satisfy

$$
\begin{aligned}
\Big(D_\mu \psi\Big)' &\equiv e^{i\phi^a t^a} \Big(D_\mu \psi\Big) \\
\therefore \qquad (\partial_\mu - igA^{a\,\prime}_\mu t^a) e^{i\phi^a t^a} \psi &= e^{i\phi^a t^a} \left(\partial_\mu - igA^a_\mu t^a\right)\psi \ . \qquad (3.18)
\end{aligned}
$$

Writing the unitary gauge rotation for compactness as $\mathcal{U} \equiv e^{i\phi^a t^a}$, this gives the transformation law for the gauge field $A^{\mu a}$ as

$$
A^{\mu a} t^a = A^{\mu a\,\prime} \left(\mathcal{U}^\dagger t^a \mathcal{U}\right) + \frac{i}{g} \mathcal{U}^\dagger (\partial_\mu \mathcal{U}) \ , \qquad (3.19)
$$

or, equivalently,

$$
A^{\mu a\,\prime} = A^{\mu a} + \frac{1}{g}(\partial^\mu \phi^a) + f^{abc} A^{\mu b} \phi^c \ . \qquad (3.20)
$$

Interestingly, for a non-Abelian gauge theory like QCD, the gauge transformation includes both the shift of $A^{\mu a}$ by a scalar-polarized mode and the rotation of the gluon color from a to b (depending on the choice of rotation angles ϕ^c).

The last ingredient in the construction of QCD is the non-Abelian field-strength tensor, from which we can build the pure gluon term. From the commutator of the covariant derivatives, we have

$$
\left[D_\mu \, , \, D_\nu\right] = \left[\partial_\mu - igA^a_\mu t^a \, , \, \partial_\nu - igA^b_\nu t^b\right]
$$

$$
\begin{aligned}
&= -ig\partial_\mu A^b_\nu t^b + ig\partial_\nu A^a_\mu t^a - g^2 A^a_\mu A^b_\nu \left[t^a\,,\, t^b\right] \\
&= -ig\partial_\mu A^b_\nu t^b + ig\partial_\nu A^a_\mu t^a - ig^2 f^{abc} A^a_\mu A^b_\nu\, t^c \\
&= -ig\big(\partial_\mu A^c_\nu - \partial_\nu A^c_\mu + g f^{abc} A^a_\mu A^b_\nu\big)\, t^c \\
\left[D_\mu\,,\, D_\nu\right] &\equiv -ig\, F^c_{\mu\nu}\, t^c\,, \qquad (3.21)
\end{aligned}
$$

where we have defined the non-Abelian field-strength tensor

$$
F^c_{\mu\nu} \equiv \partial_\mu A^c_\nu - \partial_\nu A^c_\mu + g f^{abc} A^a_\mu A^b_\nu\,. \qquad (3.22)
$$

By constructing $F^a_{\mu\nu}$ in a gauge-covariant way using (3.21), we have produced a field-strength tensor (3.22) which is more than just the free kinetic part which occurs in QCD. This is because, unlike in QED, now the free part $(\partial_\mu A^a_\nu - \partial_\nu A^a_\mu)$ is *not gauge invariant* (or even gauge covariant). Instead, the "chromo-electric" and "chromo-magnetic" fields are themselves not separately gauge invariant, transforming as

$$
F'^a_{\mu\nu} = \mathcal{U} F'^a_{\mu\nu} \mathcal{U}^\dagger\,. \qquad (3.23)
$$

While the field-strength tensor (3.22) is not gauge invariant, its *square* still is. This allows us to immediately write down the QCD Lagrangian,

$$
\begin{aligned}
\mathcal{L}_{QCD} &= \bar\psi(i\not{D} - m)\psi - \frac{1}{4} F^a_{\mu\nu} F^{\mu\nu\, a} \\
&= \bar\psi(i\not{\partial} - m)\psi - \frac{1}{4}(\partial_\mu A^a_\nu - \partial_\nu A^a_\mu)(\partial^\mu A^{\nu\, a} - \partial^\nu A^{\mu\, a}) \\
&\quad + g\bar\psi\gamma_\mu t^a \psi\, A^{\mu a} - g f^{abc}\, A^b_\mu A^c_\nu (\partial^\mu A^{\nu a}) \\
&\quad - \frac{1}{4} g^2 f^{abc} f^{ab'c'}\, A^b_\mu A^c_\nu A^{\mu\, b'} A^{\nu\, c'}\,. \qquad (3.24)
\end{aligned}
$$

The pure glue part $-\frac{1}{4} F^a_{\mu\nu} F^{\mu\nu\, a}$ and the covariant quark part $\bar\psi(i\not{D} - m)\psi$ are *separately gauge invariant*, leading to the generation of not only the quark-gluon interaction vertex $g\bar\psi\gamma_\mu t^a \psi\, A^{\mu a}$, but also to interactions among the gluons themselves through the three-gluon vertex $g\bar\psi\gamma_\mu t^a \psi\, A^{\mu a}$ and four-gluon vertex $-g f^{abc}\, A^b_\mu A^c_\nu (\partial^\mu A^{\nu a})$.

CHAPTER 4

HUGS 2022 Lecture 4: Introduction to Small-x Physics (Part 1)

4.1 Previously

- $SU(N_c)$ symmetry of the multicomponent Dirac Lagrangian
- Fundamental representation of $SU(3)$ (Gell-Mann matrices) describes quarks
- Adjoint representation (structure constants) describes gluons
- The large-N_c limit and its advantages
- Conserved color currents of $SU(N_c)$
- Non-Abelian covariant derivative and field-strength tensor
- Constructed the QCD Lagrangian

4.2 Profound Implications: The Negative Beta Function

Having constructed the QCD Lagrangian

$$\mathcal{L}_{QCD} = \bar{\psi}(i\not{D} - m)\psi - \frac{1}{4}F^a_{\mu\nu}F^{\mu\nu\,a}\,, \tag{4.1}$$

we can readily compute the Feynman rules shown in Fig. 4.1. While the quark/gluon vertex is highly similar to the equivalent QED electron/photon vertex up to a color factor, the 3-gluon and 4-gluon vertices are entirely new. Note that the 3-gluon vertex is momentum dependent, arising from its derivative coupling, while the 4-gluon vertex is momentum independent.

These new gluonic self-interactions have many profound consequences for QCD, but none is more important than their role in the QCD vacuum polarization shown in Fig. 4.2. Because of the non-Abelian nature of QCD, not only fermions (quarks) enter the virtual loops contributing to the vacuum

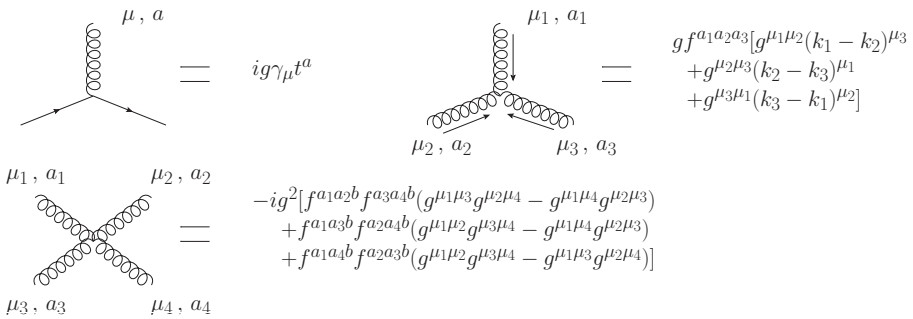

Figure 4.1: Feynman rules for the interaction vertices in QCD.

polarization; gluon loops enter as well. And the gluon loops *compete* with the quark loops: while the quarks produce a positive contribution to the beta function (as with electrons in QED), the gluons make a *negative* contribution to the beta function:

$$\beta_g = \frac{g^3}{(4\pi)^2}\left(\frac{2}{3}N_f - 11\right) , \tag{4.2}$$

where N_f is the number of quark flavors entering the loop[1]. And for $N_f = 6$ quark flavors at most, the *gluons win*, resulting in a beta function which is *negative*.

This negative beta function is the hallmark of QCD, resulting in a running coupling $\alpha_s(Q^2)$ which *decreases* with increasing momentum scale Q^2 – the *opposite* of an Abelian theory like QED. This negative beta function results in both the phenomenon of *asymptotic freedom* ($\alpha_s(Q^2) \to 0$ as $Q^2 \to \infty$) as well as *confinement* ($\alpha_s(Q^2) \to \infty$ as $Q^2 \to 0$). Unlike QED, which possesses its Landau pole in the UV limit $Q^2 \to \infty$, the negative beta function of QCD places its Landau pole in the IR regime $Q^2 \to 0$. This signifies the onset of the confinement phase transition at nonperturbative coupling in QCD in the IR, in contrast to the electroweak phase transition of QED in the UV. The other profound implication of asymptotic freedom is that *QCD is a valid, self-consistent theory up to *infinitely high* momentum scales*. What asymptotic freedom buys us is *UV completeness*: an essential property of any candidate fundamental theory of nature, which is elegantly and automatically satisfied by non-Abelian gauge theories like QCD.

4.3 Quark/Quark Scattering in Regge Kinematics

Scattering Amplitude

As an illustration of how to use the QCD Feynman rules of Fig. 4.1, let us calculate the cross section for a simple elementary process: elastic quark/quark

[1]The constants used in Eq. (4.2) are specific to $SU(3)$.

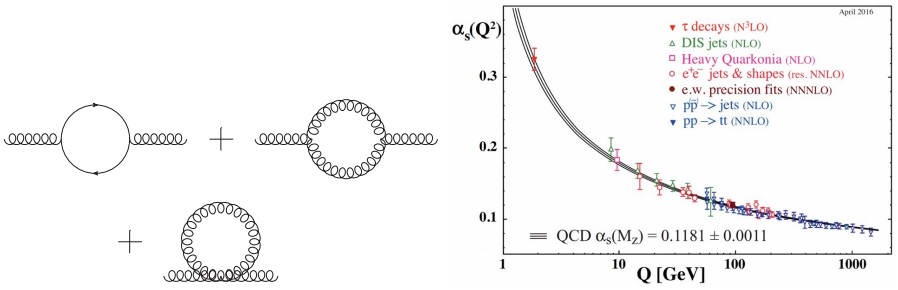

Figure 4.2: Effect of the non-Abelian vertices on the QCD running coupling.

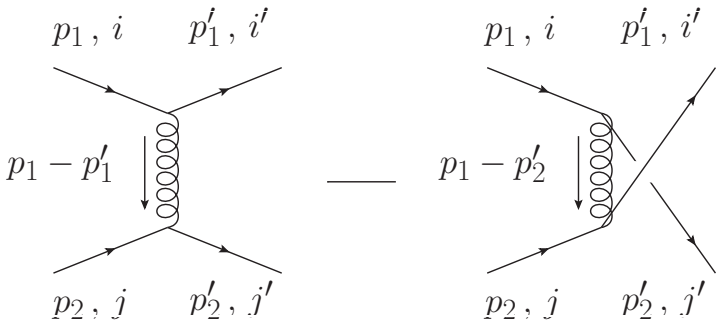

Figure 4.3: Quark-quark scattering amplitude to LO in QCD

scattering $q + q \to q + q$ in QCD as shown in Fig. 4.3. In principle there are two diagrams: the t-channel amplitude (first diagram) and the u-channel amplitude (second diagram), which differ by a minus sign due to Fermi-Dirac statistics. Here we refer to the Mandelstam variables

$$s \equiv (p_1 + p_2)^2 = (p_1' + p_2')^2\,, \tag{4.3a}$$
$$t \equiv (p_1 - p_1')^2 = (p_2' - p_2)^2\,, \tag{4.3b}$$
$$u \equiv (p_1 - p_2')^2 = (p_2 - p_1')^2\,, \tag{4.3c}$$
$$s + t + u = 4m^2\,, \tag{4.3d}$$

which compactly describe the kinematics of a $2 \to 2$ process.

From the Feynman rules of Fig. 4.1, the two amplitudes are:

$$i\mathcal{M} = i\mathcal{M}_t + i\mathcal{M}_u \tag{4.4a}$$

$$\begin{aligned} i\mathcal{M}_t &= [\bar{u}_1'\big(ig\gamma_\mu(t^a)_{i'i}\big)u_1]\left(\frac{-ig^{\mu\nu}\delta^{ab}}{t}\right)[\bar{u}_2'\big(ig\gamma_\nu(t^b)_{j'j}\big)u_2] \\ &= \frac{ig^2}{t}\,(t^a)_{i'i}(t^a)_{j'j}\,[\bar{u}_1'\gamma_\mu u_1][\bar{u}_2'\gamma^\mu u_2] \end{aligned} \tag{4.4b}$$

$$i\mathcal{M}_u = (-1)_{\text{Fermi}}[\bar{u}_1'\big(ig\gamma_\mu(t^a)_{j'i}\big)u_2]\left(\frac{-ig^{\mu\nu}\delta^{ab}}{u}\right)[\bar{u}_2'\big(ig\gamma_\nu(t^b)_{i'j}\big)u_1]$$
$$= \frac{-ig^2}{u}\,(t^a)_{j'i}(t^a)_{i'j}\,[\bar{u}_1'\gamma_\mu u_2][\bar{u}_2'\gamma^\mu u_1] \tag{4.4c}$$

High-Energy Kinematics: The Eikonal Approximation

Suppose we wish to study the behavior of the quark/quark scattering cross section in the *high-energy limit* $s \to \infty$. This is the limit relevant for high-energy collider experiments like the LHC, but we must take care to completely specify what we mean by this limit. When taking $s \to \infty$, we have two choices for what can happen to the other Mandelstam invariants. One possibility is that we increase the collision energy $s \to \infty$ and also the momentum transfer $|t| \to \infty$ proportionately. This is the *hard-scattering limit*, referred to as *Bjorken kinematics*, in which the scattering angle remains large at high energy because the exchanged momentum is growing large. In the language of deep inelastic scattering, this is the *large-x_B regime*. The other possibility is that we can take $s \to \infty$ while keeping $t = \text{const}$ fixed. This is the *forward-scattering limit*, known as *Regge kinematics*, in which the scattering angle decreases toward zero. In terms of DIS, this corresponds to the *small-x_B regime*.

Let us study the quark/quark cross section in Regge kinematics, for which

$$s \to \infty\,, \tag{4.5a}$$
$$t = \text{const}\,, \tag{4.5b}$$
$$u = 4m^2 - s - t \to -\infty\,. \tag{4.5c}$$

In this limit, the u-channel amplitude (which dominates for back-scattering, the opposite of Regge kinematics) is completely negligible, giving simply $i\mathcal{M} \approx i\mathcal{M}_t$. This is entirely natural, since the forward-scattering Regge regime is dominated by t-channel scattering.

In either Bjorken or Regge kinematics, it is very convenient to express the four-vectors in *light-front components*, defined by

$$p^\pm \equiv \frac{1}{\sqrt{2}}(p^0 \pm p^3)\,. \tag{4.6}$$

In terms of light-front components, four-vector products take the form

$$p \cdot q = p^+q^- + p^-q^+ - \vec{p}_\perp \cdot \vec{q}_\perp\,, \tag{4.7}$$

and for an on-shell particle with given p^+ and $\vec{p}_\perp$, the on-shell condition fixes the other light-front component to be

$$p^2 = 2p^+p^- - \vec{p}_\perp^{\,2} = m^2$$
$$\therefore \qquad p^- = \frac{\vec{p}_\perp^{\,2} + m^2}{2p^+}\,. \tag{4.8}$$

A particle moving at high energy along the $+z$ axis therefore has $p^+ \approx \sqrt{2}E \to \infty$ and $p^- \approx (\vec{p}_\perp^{\,2} + m^2)/(2\sqrt{2}E) \to 0$, and vice versa for a particle moving along the $-z$ axis.

Let us work in the center-of-mass frame with p_1^μ moving along the $-z$ axis and p_2^μ moving along the $+z$ axis. Then the relevant kinematics are

$$p_1^\mu \approx \left(0^+ \, , \, p_1^- \, , \, \vec{0}_\perp\right) , \tag{4.9a}$$
$$p_2^\mu \approx \left(p_2^+ \, , \, 0^- \, , \, \vec{0}_\perp\right) , \tag{4.9b}$$
$$p_1'^\mu \approx \left(0^+ \, , \, p_1^- \, , \, \vec{p}'_{1\,\perp}\right) , \tag{4.9c}$$
$$p_2'^\mu \approx \left(p_2^+ \, , \, 0^- \, , \, -\vec{p}'_{1\,\perp}\right) , \tag{4.9d}$$

where we have enforced momentum conservation $p_2' = p_1 + p_2 - p_1'$. In these high-energy kinematics, we have *approximate conservation of the separate momenta* p_1^-, p_2^+:

$$p_1'^- \approx p_1^- \tag{4.10a}$$
$$p_2'^+ \approx p_2^+ \tag{4.10b}$$
$$\tag{4.10c}$$

with only a small transverse deflection $\vec{p}'_{1\perp}$ between them. This high-energy approximation appropriate for Regge kinematics is referred to as the *eikonal approximation*.

Cross Section

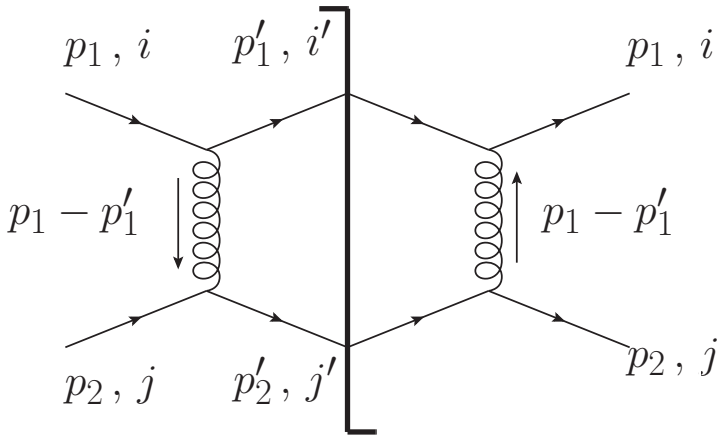

Figure 4.4: Cut-diagram representation of the amplitude-squared

Since only the t-channel amplitude contributes in Regge kinematics ("small x"), to compute the amplitude squared, summed/averaged over all quantum

numbers, we only need to consider the diagram shown in Fig. 4.4, which gives

$$\begin{aligned}
\langle \mathcal{M}^2 \rangle &\equiv \frac{1}{4} \sum_{s_1 s_1' s_2 s_2'} \frac{1}{N_c^2} \sum_{ii'jj'} (i\mathcal{M}_t)\,(i\mathcal{M}_t)^* \\
&= \frac{1}{4N_c^2} \sum_{s_1 s_1' s_2 s_2'} \sum_{ii'jj'} \left(\frac{ig^2}{t}\,(t^a)_{i'i}(t^a)_{j'j}\,[\bar{u}_1' \gamma_\mu u_1][\bar{u}_2' \gamma^\mu u_2] \right) \\
&\qquad \times \left(\frac{-ig^2}{t}\,(t^b)_{ii'}(t^b)_{jj'}\,[\bar{u}_1 \gamma_\nu u_1'][\bar{u}_2 \gamma^\nu u_2'] \right) \\
&= \frac{1}{4N_c^2} \frac{g^4}{t^2} \sum_{ii'jj'} (t^a)_{i'i}(t^b)_{ii'}(t^a)_{j'j}(t^b)_{jj'} \\
&\qquad \times \sum_{s_1 s_1'} [\bar{u}_1' \gamma_\mu u_1][\bar{u}_1 \gamma_\nu u_1'] \sum_{s_2 s_2'} [\bar{u}_2' \gamma^\mu u_2][\bar{u}_2 \gamma^\nu u_2'] \\
&= \frac{1}{4N_c^2} \frac{g^4}{t^2} \mathrm{tr}[t^a t^b]\,\mathrm{tr}[t^a t^b] \mathrm{tr}[\not{p}_1' \gamma_\mu \not{p}_1 \gamma_\nu] \mathrm{tr}[\not{p}_2' \gamma^\mu \not{p}_2 \gamma^\nu]\,. \qquad (4.11)
\end{aligned}$$

The spin sums are converted into traces in the usual way, as in QED[2], while the color traces can be evaluated for general N_c using the identities

$$\mathrm{tr}[t^a t^b] = \frac{1}{2}\delta^{ab}\,, \qquad (4.12a)$$

$$t^a t^a = C_f \mathbf{1} \equiv \frac{N_c^2 - 1}{2N_c}\mathbf{1}\,, \qquad (4.12b)$$

$$\mathrm{tr}[\mathbf{1}] = N_c\,, \qquad (4.12c)$$

giving

$$\mathrm{tr}[t^a t^b]\,\mathrm{tr}[t^a t^b] = \frac{1}{2}\mathrm{tr}[t^a t^a] = \frac{1}{2} C_F \mathrm{tr}[\mathbf{1}] = \frac{N_c C_F}{2}\,. \qquad (4.13)$$

Then the amplitude squared is

$$\begin{aligned}
\langle \mathcal{M}^2 \rangle &= \frac{4}{N_c^2} \frac{g^4}{t^2} \frac{N_c C_F}{2} \Big(p_1'^{\mu} p_1^{\nu} + p_1'^{\nu} p_1^{\mu} - (p_1 \cdot p_1') g^{\mu\nu} \Big) \Big(p_2'^{\mu} p_2^{\nu} + p_2'^{\nu} p_2^{\mu} - (p_2 \cdot p_2') g^{\mu\nu} \Big) \\
&= \frac{4g^4}{t^2} \frac{C_F}{2N_c} \Big(2(p_1 \cdot p_2)(p_1' \cdot p_2') + 2(p_1 \cdot p_2')(p_2 \cdot p_1') - 4(p_1 \cdot p_1')(p_2 \cdot p_2') \Big)
\end{aligned}$$

[2]Here we use the massless approximation for the quarks, which is appropriate for high-energy kinematics.

$$= \frac{4g^4}{t^2}\frac{C_F}{2N_c}\left(2(\tfrac{s}{2})^2 + 2(-\tfrac{u}{2})^2 - 4(-\tfrac{t}{2})^2\right)$$

$$\approx \frac{4g^4}{t^2}\frac{C_F}{2N_c}\left(2(\tfrac{s}{2})^2 + 2(+\tfrac{s}{2})^2\right)$$

$$\langle \mathcal{M}^2 \rangle \approx 4g^4 \frac{C_F}{2N_c}\frac{s^2}{t^2} \tag{4.14}$$

where we have simplified the kinematics according to the Regge limit.

Given this expression for the amplitude squared, the corresponding differential cross section is

$$d\sigma = \frac{1}{2E_1 2E_2 |\vec{v}_1 - \vec{v}_2|}\frac{d^3p_1'}{(2\pi)^3 2E_1'}\frac{d^3p_2'}{(2\pi)^3 2E_2'}\langle \mathcal{M}^2 \rangle (2\pi)^4\,\delta^4(p_1 + p_2 - p_1' - p_2')\,. \tag{4.15}$$

In Regge kinematics, the flux prefactor is

$$\frac{1}{2E_1 2E_2 |\vec{v}_1 - \vec{v}_2|} = \frac{1}{8E_1E_2} = \frac{1}{4p_1^- p_2^+} = \frac{1}{4p_1 \cdot p_2} = \frac{1}{2s}\,, \tag{4.16}$$

and we can change variables to light-front coordinates in the phase space and delta function, giving

$$d\sigma = \frac{1}{2s}\frac{d^2p_{1\perp}'\,dp_1'^-}{2p_1'^-}\frac{d^2p_{2\perp}'\,dp_2'^+}{2p_2'^+}\frac{\langle \mathcal{M}^2 \rangle}{(2\pi)^2}\delta(p_2^+ - p_2'^+)\delta(p_1^- - p_1'^-)\delta(\vec{p}_{1\perp}' + \vec{p}_{2\perp}')\,. \tag{4.17}$$

We can exhaust the constraints of the delta function by integrating over $p_1'^-$, $p_2'^+$, and $\vec{p}_2'$ to obtain

$$\begin{aligned}\frac{d\sigma}{d^2p_{1\perp}'} &= \frac{1}{2s}\frac{1}{4p_1^- p_2^+}\frac{\langle \mathcal{M}^2 \rangle}{(2\pi)^2} \\ &= \frac{1}{(2s)^2}\frac{\langle \mathcal{M}^2 \rangle}{(2\pi)^2}\,.\end{aligned} \tag{4.18}$$

Finally, we insert the expression (4.14) for the amplitude squared, obtaining

$$\frac{d\sigma}{d^2p_{1\perp}'} = 4\alpha_s^2\frac{C_F}{2N_c}\frac{1}{p_{1\perp}'^4}\,. \tag{4.19}$$

in terms of $\alpha_s \equiv g^2/4\pi$ and using $t \approx -p_{1\perp}'^2$. For QCD with $N_c = 3$, we have $C_F = 4/3$ and $\frac{C_F}{2N_c} = \frac{2}{9}$.

The eikonal approximation (high-energy / small-x / Regge kinematics) has substantially simplified the cross section (4.19). Most importantly, the cross

section for t-channel scattering at high energies is *unsuppressed as* $s \to \infty$. This is a general feature of high-energy scattering: the interactions are dominated by the exchange of vector bosons (such as gluons). Other processes mediated by the exchange of quarks (or even scalars in the case of scalar QCD) are suppressed by powers of s as $s \to \infty$, such that *eikonal scattering is always dominated by gluon exchange*. The gluons which mediate this high-energy scattering exchange no p_1^- or p_2^+ momenta between the high-energy quarks, essentially carrying only transverse momenta:

$$q^\mu \equiv (p_1 - p_1')^\mu \approx \left(0^+ \, , \, 0^- \, , \, -\vec{p}_{1\perp}'\right) . \tag{4.20}$$

These exchanged transverse gluons are referred to as *Glauber gluons* or *Coulomb gluons*, for which the only relevant dynamics is transverse to the eikonal collision axis.

CHAPTER 5

HUGS 2022 Lecture 5: Introduction to Small-x Physics (Part 2)

5.1 Previously

- QCD Feynman rules
- QCD negative beta function: asymptotic freedom / confinement
- QCD as our best template for a UV-complete theory of nature
- Regge kinematics ($s \gg |t| \gg \Lambda^2_{QCD}$) vs. Bjorken kinematics ($s \sim |t| \gg \Lambda^2_{QCD}$)
- Light-front coordinates $p^\pm$
- t-channel quark/quark scattering in the eikonal approximation
- Gluon-mediated scattering is unsuppressed by s as $s \to \infty$

5.2 Radiative Corrections: Soft QCD Bremsstrahlung

Having computed the cross section for elastic $2 \to 2$ scattering of quarks ($q + q \to q + q$) in eikonal kinematics, let us next proceed to study *particle production* in this limit. The dominant mechanism of particle production in eikonal kinematics is the radiation of *soft gluon bremsstrahlung* as an NLO correction to the elastic scattering cross section we computed previously.

The Feynman diagrams generating the leading contribution to $q+q \to q+q+g$ are shown in Fig. 5.1. There are 5 diagrams in total. Four of them (A-D) are totally analogous to the radiation of soft photons in QED; they consist of initial- and final-state radiation which can be emitted either from the "projectile" (p_1) or the "target" (p_2). The last diagram (E) is uniquely non-Abelian, in which the *exchanged gluon itself* undergoes bremsstrahlung.

As before, let us consider the case of eikonal scattering in Regge kinematics: p_1^- , $p_2^+ \sim \sqrt{s} \to \infty$. We will moreover focus on the case when the radiated

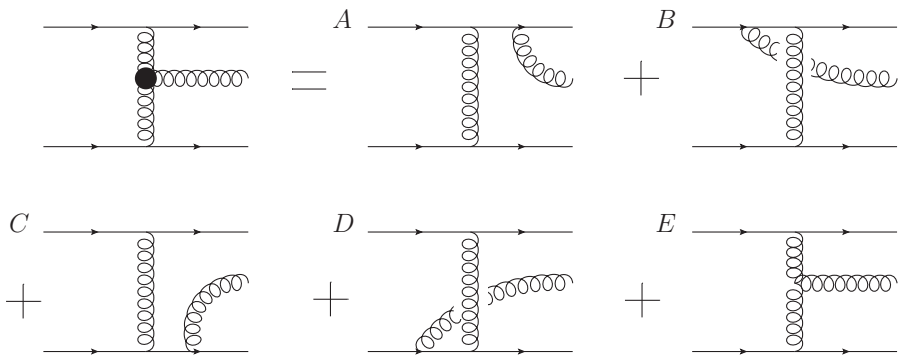

Figure 5.1: Feynman diagrams contributing to the scattering amplitude $i\mathcal{M}$ for the $2 \to 3$ radiative process $q + q \to q + q + g$. The sum of all the diagrams is represented by the thick effective vertex on the left, known as the *Lipatov vertex*.

gluon is "longitudinally soft," meaning that its light-front momenta k^+, k^- are both small compared to the momenta of the incoming particles:

$$p_1^- \gg k^- \gg p_2^- \,, \tag{5.1a}$$

$$p_2^+ \gg k^+ \gg p_1^+ \,. \tag{5.1b}$$

When expressed in terms of the *rapdity*

$$y = \frac{1}{2} \ln \frac{k^+}{k^-} \tag{5.2}$$

this means that we are looking at particle production at *mid-rapidity* $y_2 \gg y \gg y_1$. Particle production in this regime preserves the eikonal approximation because the radiated gluon does not disturb the flow of large p_1^- and p_2^+ through the diagram. This limit is also the limit in which the longitudinal momentum fraction called (Feynman) x is small:

$$x_F \equiv \frac{k^+}{p^+} \ll 1 \,. \tag{5.3}$$

This is one of the meanings of "small x physics."

Initial- vs. Final-State Radiation: Kinematics

Let us now compute in detail the final- and initial-state radiation diagrams A and B shown in Fig. 5.2. First let us specify the kinematics. For the incoming particles we have the same setup as before:

$$p_1^\mu = \left(0^+ \,,\, p_1^- \,,\, \vec{0}_\perp\right) \,, \tag{5.4a}$$

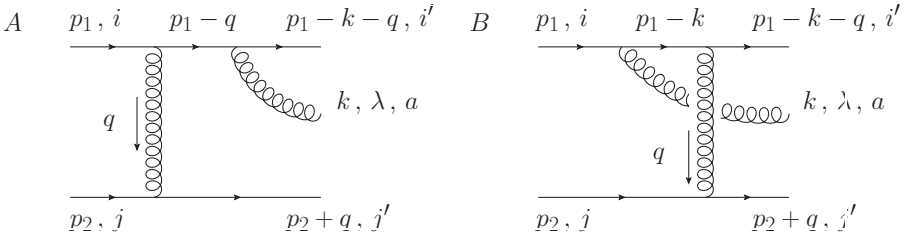

Figure 5.2: Initial-state (B) and final-state (A) radiation amplitudes for bremsstrahlung off the "projectile" p_1.

$$p_2^\mu = \left(p_2^+\,,\,0\,,\,\vec{0}_\perp\right)\,, \tag{5.4b}$$

while the momenta k^μ, q^μ are constrained by the on-shell conditions of the 3 final-state particles. For k^μ this gives

$$k^\mu = \left(k^+\,,\,\frac{k_\perp^2}{2k^+}\,,\,\vec{k}_\perp\right)\,, \tag{5.5}$$

and for q^μ we deduce the values of $q^\pm$ from the on-shell conditions of the outgoing quarks:

$$\begin{aligned} q^+ &= p_1^+ - k^+ - (p_1-k-q)^+ \\ &\approx -k^+\,, \end{aligned} \tag{5.6a}$$

$$\begin{aligned} q^- &= (p_2+q)^- - p_2^- \\ q^- &\approx \frac{q_\perp^2}{2p_2^+}\,. \end{aligned} \tag{5.6b}$$

Altogether, this gives the eikonal kinematics as

$$p_1^\mu = \left(0^+\,,\,p_1^-\,,\,\vec{0}_\perp\right)\,, \tag{5.7a}$$

$$p_2^\mu = \left(p_2^+\,,\,0\,,\,\vec{0}_\perp\right)\,, \tag{5.7b}$$

$$k^\mu = \left(k^+\,,\,\frac{k_\perp^2}{2k^+}\,,\,\vec{k}_\perp\right)\,, \tag{5.7c}$$

$$q^\mu = \left(-k^+\,,\,\frac{q_\perp^2}{2p_2^+}\,,\,\vec{q}_\perp\right)\,. \tag{5.7d}$$

With the eikonal kinematics (5.7), it is straightforward to compute the virtualities of the intermediate-state particles for diagrams A and B. The exchanged gluon is the same for both diagrams:

$$\begin{aligned} q^2 &= 2q^+q^- - q_\perp^2 \\ &= -\frac{k^+}{p_2^+}q_\perp^2 - q_\perp^2 \\ &\approx -q_\perp^2\,, \end{aligned} \tag{5.8}$$

just as with the elastic scattering process we computed before. The intermediate quark propagators are different for the two diagrams, giving

$$\begin{aligned}(p_1-q)^2 &= 2(p_1^+-q^+)(p_1^- - q^-) - (\vec{p}_{1\perp}-\vec{q}_\perp)^2 \\ &\approx 2(0^+ + k^+)(p_1^- - \frac{q_\perp^2}{2p_2^+}) - q_\perp^2 \\ (p_1-q)^2 &\approx 2k^+p_1^- \,, \end{aligned} \tag{5.9a}$$

$$\begin{aligned}(p_1-k)^2 &= 2(p_1^+-k^+)(p_1^- - k^-) - (\vec{p}_{1\perp}-\vec{q}_\perp)^2 \\ &\approx 2(0^+ - k^+)(p_1^- - \frac{k_\perp^2}{2k^+}) - q_\perp^2 \\ &\approx -2k^+p_1^- \,. \end{aligned} \tag{5.9b}$$

Crucially, the virtualities of these two intermediate states are *exactly opposite* in the high-energy limit, and this virtuality is small compared to the collision energy s:

$$(p_1-q)^2 = -(p_1-k)^2 = 2k^+p_1^- \qquad \ll \qquad 2p_2^+p_1^- = s \,. \tag{5.10}$$

This shows that the *kinematics of the two diagrams are identical, but different by a sign* accounting for the fact that the propagator is timelike for diagram A but spacelike for diagram B.

Initial- vs. Final-State Radiation: Amplitudes

The evaluation of the amplitudes for diagrams A and B is now straightforward. For diagram A we have

$$\begin{aligned} i\mathcal{M}_A = [\bar{u}_1'\big(ig\not{\epsilon}^*_\lambda(t^a)_{i'i''}\big)\left(\frac{i(\not{p}_1-\not{q})}{(p_1-q)^2}\right)\big(ig\gamma_\mu(t^b)_{i''i}\big)u_1] \\ \times\left(\frac{-ig^{\mu\nu}\delta^{bb'}}{q^2}\right)[\bar{u}_2'\big(ig\gamma_\nu(t^{b'})_{j'j}\big)u_2] \end{aligned}$$

$$= \frac{+ig^3}{q_\perp^2\,(2k^+p_1^-)}(t^at^b)_{i'i}(t^b)_{j'j}[\bar{u}_1'\not{\epsilon}^*_\lambda(\not{p}_1-\not{q})\gamma_\mu u_1][\bar{u}_2'\gamma^\mu u_2] \,. \tag{5.11}$$

Rather than proceeding to square this amplitude (with all the messy interferences), let us proceed to evaluate the numerator algebra in the eikonal approximation here, at the amplitude level. For instance, both the incoming momentum p_2 and outgoing momentum $p_2' = p_2 + q$ are overwhelmingly dominated by the light-front component $p_2^+ \to \infty$. Since $p_2^\mu \approx p_2'^\mu \approx (p_2^+, 0^-, \vec{0}_\perp)$, we can employ the simplified version of the Gordon identity[1]

$$[\bar{u}_{ps}\gamma^\mu u_{ps'}] = 2p^\mu\,\delta_{ss'} \tag{5.12}$$

[1]Note that here we consider the forward limit of the matrix element $p' = p$. The full form of the Gordon identity also includes other terms proportional to $(p-p')$.

to directly evaluate the spinor product for the target:

$$[\bar{u}_2'\gamma^\mu u_2] \approx 2p_2^+\,\delta^\mu{}_+\,\delta_{s_2s_2'}\,. \tag{5.13}$$

This sets $\mu = +$ in the spinor matrix element for the projectile (note that $\gamma_+ = \gamma^-$), and we can further eikonalize the spinor matrix element:

$$\begin{aligned}
[\bar{u}_1'\not{\epsilon}_\lambda^*(\not{p}_1 - \not{q})\gamma^- u_1] &\approx p_1^-[\bar{u}_1'\not{\epsilon}_\lambda^*\gamma^+\gamma^- u_1] \\
&= p_1^-[\bar{u}_1'\not{\epsilon}_\lambda^*\{\gamma^+,\gamma^-\}u_1] \\
&= 2p_1^-[\bar{u}_1'\not{\epsilon}_\lambda^* u_1] \\
&= 2p_1^-(\epsilon_\lambda^*)_\mu[\bar{u}_1'\gamma^\mu u_1] \\
&\approx 2p_1^-(\epsilon_\lambda^*)_\mu(2p_1^-\,\delta^\mu{}_-\,\delta_{s_1s_1'}) \\
&= (2p_1^-)^2(\epsilon_\lambda^*)^+\delta_{s_1s_1'}
\end{aligned} \tag{5.14}$$

where we have used the Dirac equation

$$\begin{aligned}
\not{p}_1 u_1 = p_1^-\gamma^+ u_1 &= 0 \\
\therefore \qquad \gamma^+ u_1 &= 0
\end{aligned} \tag{5.15}$$

for the incoming quark. Substituting these results back into (5.11) gives

$$i\mathcal{M}_A = \frac{+ig^3}{q_\perp^2\,(2k^+p_1^-)}(t^at^b)_{i'i}(t^b)_{j'j}\big(2p_2^+\,\delta_{s_2s_2'}\big)\big((2p_1^-)^2(\epsilon_\lambda^*)^+\delta_{s_1s_1'}\big)$$

$$= ig^3\frac{2s}{q_\perp^2}\frac{(\epsilon_\lambda^*)^+}{k^+}\,(t^at^b)_{i'i}(t^b)_{j'j}\,\delta_{s_1s_1'}\,\delta_{s_2s_2'}\,. \tag{5.16}$$

In a similar way, we can evaluate amplitude B in the eikonal approximation:

$$\begin{aligned}
i\mathcal{M}_B = [\bar{u}_1'\big(ig\gamma_\mu(t^b)_{i'i''}\big)&\left(\frac{i(\not{p}_1 - \not{k})}{(p_1-k)^2}\right)\big(ig\not{\epsilon}_\lambda^*(t^a)_{i''i}\big)u_1] \\
&\times\left(\frac{-ig^{\mu\nu}\delta^{bb'}}{q^2}\right)[\bar{u}_2'\big(ig\gamma_\nu(t^{b'})_{j'j}\big)u_2]
\end{aligned}$$

$$= \frac{+ig^3}{q_\perp^2\,(-2k^+p_1^-)}\,(t^bt^a)_{i'i}(t^b)_{j'j}\,[\bar{u}_1'\gamma_\mu(\not{p}_1 - \not{k})\not{\epsilon}_\lambda^* u_1][\bar{u}_2'\gamma^\mu u_2]$$

$$= \frac{+ig^3}{q_\perp^2\,(-2k^+p_1^-)}\,(t^bt^a)_{i'i}(t^b)_{j'j}\,[\bar{u}_1'\gamma^-(\not{p}_1 - \not{k})\not{\epsilon}_\lambda^* u_1](2p_2^+\,\delta_{s_2s_2'})$$

$$= -ig^3\frac{2p_1^-p_2^+}{q_\perp^2}\frac{1}{2k^+p_1^-}\,(t^bt^a)_{i'i}(t^b)_{j'j}\,\delta_{s_2s_2'}\,[\bar{u}_1'\gamma^-\gamma^+\not{\epsilon}_\lambda^* u_1]$$

$$= -ig^3 \frac{2s}{q_\perp^2} \frac{1}{2k^+ p_1^-} (t^b t^a)_{i'i} (t^b)_{j'j} \, \delta_{s_2 s_2'} \, [\bar{u}_1' \not{\epsilon}_\lambda^* u_1]$$

$$i\mathcal{M}_B = -ig^3 \frac{2s}{q_\perp^2} \frac{(\epsilon_\lambda^*)^+}{k^+} (t^b t^a)_{i'i} (t^b)_{j'j} \, \delta_{s_1 s_1'} \delta_{s_2 s_2'} \, . \tag{5.17}$$

Discussion

Comparing the final-state radiation diagram $i\mathcal{M}_A$ from Eq. (5.16) with the inital-state radiation diagram $i\mathcal{M}_B$, from Eq. (5.17), we make several interesting observations:

- These two amplitudes are *almost identical*, owing to the eikonal kinematics of the Regge scattering. The dependence on all kinematic variables is the same.
- The amplitudes are proportional to $1/k^+$, and since $k^+ \ll p_2^+$ is a soft momentum scale, the amplitude to radiate a soft gluon is *parametrically large*.
- The eikonal limit is in general *spin-independent*. This means we must work harder and include *sub-eikonal corrections* if we want to describe the behavior of *spin asymmetries* in Regge kinematics.
- The two amplitudes differ by a minus sign. This sign difference came from Eq. (5.10), arising because the *only* kinematic difference between the two amplitudes is that for diagram A, the propagator is timelike (k^+ and p_1^- flowing in the same direction), while for diagram B, it is spacelike (k^+ and p_1^- flowing in opposite directions).
- Aside from the minus sign, the only other difference between the two amplitudes is the *order of the two color rotations* of the projectile quark. For diagram A, the scattering occurs before the radiation, leading to the combined color rotation $(t^a t^b)_{i'i}$. For diagram B, the radiation vertex occurs first, leading to $(t^b t^a)_{i'i}$
- In the eikonal approximation, both amplitudes to radiate the gluon from the projectile are proportional to the polarization vector $(\epsilon_\lambda^*)^+$. This means that if we strategically *choose a gauge* such that $(\epsilon_\lambda^*)^+ = 0$ (the light-front gauge $A^+ = 0$), then $i\mathcal{M}_A = i\mathcal{M}_B = 0$. This allows us to *suppress radiation from the projectile in this special gauge*, leaving only contributions from the other diagrams C, D, E. The same is true for the target: choosing the light-front gauge $A^- = 0$ suppresses radiation from the target, resulting in $i\mathcal{M}_C = i\mathcal{M}_D = 0$. An appropriate choice of gauge like this can drastically simplify the calculation.

- Diagrams C and D, being mirror images of A and B, can be trivially obtained from Eqs. (5.16) and (5.17) by appropriate *substitution of the momenta*.

Understanding the general form of the bremsstrahlung amplitude in eikonal kinematics leads to a profound difference between the radiation pattern produced by QED and by QCD. Adding the two amplitudes together, we obtain

$$\begin{aligned} i\mathcal{M}_A + i\mathcal{M}_B &= ig^3 \frac{2s}{q_\perp^2} \frac{(\epsilon_\lambda^*)^+}{k^+} \left((t^a t^b)_{i'i} - (t^b t^a)_{i'i} \right) (t^b)_{j'j} \, \delta_{s_1 s_1'} \, \delta_{s_2 s_2'} \\ &= ig^3 \frac{2s}{q_\perp^2} \frac{(\epsilon_\lambda^*)^+}{k^+} \left[t^a, t^b \right]_{i'i} (t^b)_{j'j} \, \delta_{s_1 s_1'} \, \delta_{s_2 s_2'} \\ &= ig^3 \frac{2s}{q_\perp^2} \frac{(\epsilon_\lambda^*)^+}{k^+} \left(i f^{abc} (t^c)_{i'i} \right) (t^b)_{j'j} \, \delta_{s_1 s_1'} \, \delta_{s_2 s_2'} \\ &= -g^3 \, f^{abc} (t^c)_{i'i} (t^b)_{j'j} \, \frac{2s}{q_\perp^2} \frac{(\epsilon_\lambda^*)^+}{k^+} \, \delta_{s_1 s_1'} \, \delta_{s_2 s_2'} \, . \end{aligned} \tag{5.18}$$

The relative minus sign between the initial-state- and final-state-radiation diagrams, together with the reversed order of the color rotations, has produced a *commutator* of the color matrices. This changes the combined color structure to something proportional to the structure constants f^{abc} – exactly of the same form as diagram E containing the triple-gluon vertex. Thus all of the diagrams A-E can be combined into a single structure with an effective 3-gluon vertex, known as the *Lipatov vertex*, as depicted in Fig. 5.1.

The difference here between QED and QCD could not be more pronounced. In QCD, the initial-state radiation diagrams combine with the final-state radiation diagrams in a systematic way, leading to parametrically large rate of particle production at high energies. But in QED, without the presence of the non-Abelian $SU(N_c)$ generators, the *amplitudes simply cancel instead*, and diagram E does not exist. For electron/electron scattering in QED at high energies, *no net photon radiation is produced*, and the Regge limit is trivial and uninteresting. This just corresponds to the familiar semi-classical statement that an electron must *accelerate* to produce radiation, and since $s \to \infty$ with t fixed, the scattering angle goes to zero and the electrons do not accelerate. But in QCD, the quarks have an internal color degree of freedom as well as their kinematic variables. Unlike electrons, quarks can "accelerate" in color space, leading to a proliferation of soft gluon radiation at mid rapidity. Thus the high-energy Regge limit (small x_F) is *uniquely sensitive to the non-Abelian nature of QCD*. And, moreover, *any non-Abelian gauge theory* (not just QCD) will produce an abundance of soft gluon radiation – directly as a consequence of the non-commutative vertex.

Cross Section

A complete calculation of all the diagrams in Fig. 5.1 leads to the full amplitude

$$i\mathcal{M} = -g^3\, f^{abc}(t^c)_{i'i}(t^b)_{j'j}\frac{4s}{q_\perp^2}\;(\epsilon^*_\lambda)_\mu\left(\frac{k_\perp^\mu}{k_\perp^2} - \frac{(k+q)_\perp^\mu}{(k+q)_\perp^2}\right). \tag{5.19}$$

As promised, this diagram has the color structure of the 3-gluon vertex, along with a characteristic transverse momentum dependence which defines the Lipatov vertex. Squaring the amplitude and summing/averaging over the spin and color quantum numbers yields

$$\langle|\mathcal{M}|^2\rangle = 8g^3C_F\frac{s^2}{q_\perp^2\,k_\perp^2\,(k+q)_\perp^2} \tag{5.20}$$

and to the differential cross section

$$\frac{d\sigma}{d^2k_\perp\,d^2q_\perp\,dy} = \frac{2\alpha_s^3C_F}{\pi^2}\frac{1}{q_\perp^2\,k_\perp^2\,(k+q)_\perp^2}\,. \tag{5.21}$$

Some features of this cross section, like its transverse momentum dependence, are specific to the choice of quark/quark scattering. These will be modified in more realistic choices of in/out states, such as color-neutral dipoles or real protons. But the *rapidity (in)dependence* of the cross section is quite generic, following simply from the eikonal approximation and the form of the quark/gluon vertex in QCD.[2]

The result is that leading-order QCD predicts a *spectrum of soft gluon radiation which is uniform at mid-rapidity*:

$$\frac{dN_g}{dy} \propto \frac{d\sigma}{dy} = \text{const}\,, \tag{5.22}$$

which is exactly what is seen experimentally from particle production at mid-rapidity in high-energy hadronic collisions (Fig. 5.3). We find that *QCD produces an abundance of soft gluon radiation at high energies* which is *boost-invariant* (rapidity-independent) at leading power in the eikonal expansion.

Even more profoundly, that constancy of the gluon spectrum with rapidity sets up a dynamic *competition* between the parametrically *small probability* to emit a gluon in perturbative QCD ($\alpha_s \ll 1$) and the *large phase space* of rapidity available to the gluon. For the inclusive cross section $q+q \to q+q+X$ where X can be anything, the $q+q \to q+q+g$ cross section is an NLO correction to the elastic process $q+q \to q+q$. This nominally NLO correction is suppressed by a factor of α_s compared to the elastic process, but it is enhanced by an integral over the available rapidity window between the rapidity Y_1 of the projectile and the rapidity Y_2 of the target:

$$\frac{\sigma_{qq\to qqg}}{\sigma_{qq\to qq}} \sim \alpha_s\int_{Y_1}^{Y_2} dy = \alpha_s(Y_2 - Y_1)\,. \tag{5.23}$$

[2] The same rapidity independence also arises from bremsstrahlung emitted from eikonal gluons.

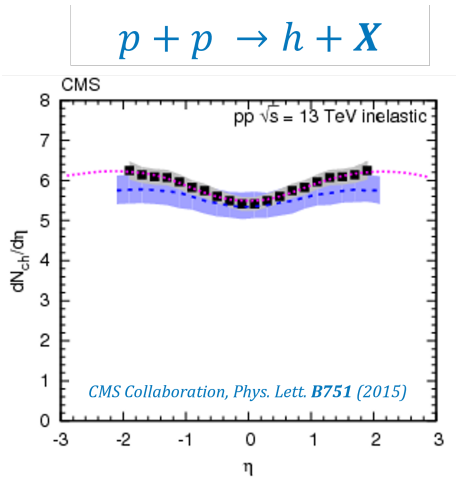

Figure 5.3: A uniform distribution of hadrons at mid-rapidity measured by the CMS Collaboration, in excellent agreement with our expectations from the tree-level calculation in QCD.

That rapidity interval is

$$\begin{aligned} Y_2 - Y_1 &= \frac{1}{2}\ln\frac{p_2^+}{p_2^-} - \frac{1}{2}\ln\frac{p_1^+}{p_1^-} \\ &= \frac{1}{2}\ln\frac{p_1^- p_2^+}{p_1^+ p_2^-} \\ &= \frac{1}{2}\ln\frac{(s/2)}{(m^4/2s)} \\ &= \ln\frac{s}{m^2}\,, \end{aligned} \tag{5.24}$$

so that the total contribution of the soft gluon bremsstrahlung to the inclusive cross section is

$$\frac{\sigma_{qq\to qqg}}{\sigma_{qq\to qq}} \sim \alpha_s \ln\frac{s}{m^2}\,. \tag{5.25}$$

If the center-of-mass energy s is large, but not exponentially large, $\ln\frac{s}{m^2} \sim \mathcal{O}(1)$ and the correction (5.25) is just a small NLO correction to the elastic process, consistent with perturbation theory. But if s becomes exponentially larger than m^2, then $\ln\frac{s}{m^2} \gg 1$ begins to compete with the smallnes of the coupling constant α_s. When the phase space becomes sufficiently large that

$$\alpha_s \ln\frac{s}{m^2} \sim 1 \tag{5.26}$$

then the NLO bremsstrahlung amplitude is *of the same order* as the LO elastic process. And *two sequential emissions* of appropriately soft bremsstrahlung are

also of the same order as the LO process. And so on, for any number of soft gluon emissions. In this limit, describing a *cascade of small-x_F gluons*, the large logarithms must be *resummed to all orders*. This results in a massive increase in the gluon density and in the abundance of particle production at high energies (synonymous with small x). The differential equation which expresses that leading-logarithmic resummation of soft gluon emission is known as the BFKL equation (Balitsky-Fadin-Kuraev-Lipatov), and its prediction of rapidly growing gluon densities in hadronic systems drives high-energy QCD toward the limit of nonlinear, high-density physics.